Available online at www.sciencedirect.com
ScienceDirect
Energy Procedia 69 (2015) 779 – 789
Energy Procedia

International Conference on Concentrating Solar Power and Chemical Energy Systems, SolarPACES 2014

The design and numerical study of a 2MWh molten salt thermocline tank

ZS Chang [a, b], X Li [a,*], C Xu [c], C Chang [a], ZF Wang [a]

[a] *Key Laboratory of Solar Thermal Energy and Photovoltaic System, Institute of Electrical Engineering, Chinese Academy of Sciences, Beijing 100190, China*
[b] *University of Chinese Academy of Sciences, Beijing 100049, China*
[c] *North China Electric Power University, Beijing, 100190, China*

Abstract

The two tank molten salt thermal storage system is widely used in the commercialized solar thermal power plant. However, the thermocline storage system with a low-cost filler material is a more economically feasible option. In this study, a transient two-dimensional and two-temperature model is developed to investigate the heat transfer and fluid dynamics in a molten salt thermocline thermal storage system. After model validation, the effects of inlet flow boundary condition and storage medium properties including fluid and solid materials on the thermal performance of thermocline storage system are investigated. The results show that thermoclne thickness increases slowest with solar salt as heat transfer fluid (HTF) and Cofalit® as solid material in the thermocline tank. Any non-uniformity in the inlet velocity flow would only enhance mixing and widen the thermocline appreciably, which contributes to the loss of thermodynamic availability of stored energy. The thermocline thickness increases with the non-uniformity of the inlet velocity boundary condition. So smaller non-uniformity of inlet flow is better in non-uniform flow though it may causes larger fluctuations in average outlet temperature. Smaller inlet mass flow rate is better for the thermocline storage tank, while it also causes smaller discharging power. With the chosen basic design parameters such as fluid and solid materials, the size of a 2MWh thermocline tank is determined by a simple one-dimensional design method. Tank with larger H/D ratio has higher discharge efficiency. It helps to figure out the thermal stratification mechanism of a storage tank and thereby to determine optimum design and operating conditions.

Peer review by the scientific conference committee of SolarPACES 2014 under responsibility of PSE AG

* Corresponding author. Tel.: +86-010-62558289.
E-mail address: drlixin@mail.iee.ac.cn

Peer review by the scientific conference committee of SolarPACES 2014 under responsibility of PSE AG
doi:10.1016/j.egypro.2015.03.094

Keywords: molten salt; thermocline; design; fluid and solid materials; non-uniform inlet flow

1. Introduction

Power generation using concentrated solar power plants (CSP) is one of the several promising, emerging renewable energy technologies. The advantage of CSP systems relative to other utility scale renewable energy technologies is the ability to store energy as high temperature heat and continue producing power when solar energy is not available. A lot of research efforts have been recently focused on the integration of solar thermal energy storage (TES) as a viable means to enhance dispatchability, increase the value of concentrated solar energy and make the plant more reliable.

Nomenclature

C_p	specific heat capacity, J/kg·K	V	velocity, m/s
D	diameter of the tank, m	**Greek symbols**	
d_p	diameter of the solid filler, m	ε	porosity of packed-bed region
$\vec{e}_r$, $\vec{e}_x$	unit vector in the r and x direction, respectively	η	efficiency
F	inertial coefficient	μ	viscosity, kg/m·s
g	acceleration due to gravity, m/s^2	ρ	density, kg/m^3
H	tank height, m	**subcripts**	
h_i	interstitial heat transfer coefficient, W/m^3·K	air	air
K	permeability of porous material, m^2	crit	critical value
k	thermal conductivity, W/m·K	c	cold fluid
l	length, m	dc	discharging
$\dot{m}$	mass flow rate, kg/s	eff	effective value
Nu	Nusselt number	h	hot fluid
P	thermal power, W	i	insulation layers or tank steel
p	pressure, Pa	in	inlet
Pr	Prandtl number	l	length
Q	heat, J	out	outlet
Re	Reynolds number	s	solid material
T	temperature, K	st	steel wall
t	time, s	store	energy stored

There are a number of viable candidates for TES systems that might be developed and applied on a commercial scale for CSP plants. Presently, sensible molten salt TES systems including two-tank system and one-tank thermocline system are widely applied or under development worldwide [1], as molten salt used as the storage medium and direct heat transfer fluid can offer the best balance of capacity, cost, efficiency and usability at high temperatures [7]. The two-tank system has a high-temperature tank and a low-temperature tank for storing molten salt. It is the most mature utility-scale TES system for CSP plants, and has been applied or projected in many CSP plants. However, the two-tank molten salt TES system has very limited space for cost reduction. The one-tank thermocline system has only one storage tank and would use molten salt as the direct heat transfer fluid, storing energy gathered in the solar field, and transferring that energy when needed. With the hot and cold fluid in a single tank, the thermocline storage system relies on thermal buoyancy to maintain thermal stratification and discrete high- and low-temperature regions of the TES system. A low-cost filler material used to pack the single storage tank acts

as the primary thermal storage medium and reduces the overall required quantities of the relatively higher cost molten salt heat transfer fluid. As thus the one-tank thermocline system provides a more cost-effective option for TES systems with a potential cost reduction of 20%-37% compared to the two-tank system [1]. The one-tank thermocline system has been investigated and developed worldwide recently. A small pilot-scale packed-bed molten salt thermocline system has been successfully demonstrated in Sandia National Laboratories [10]. M. M. Valmiki et al. presents an experimental study of the energy charge and discharge processes in a small oil packed bed thermocline thermal storage tank [17]. Some research efforts have led to the development of nitrate salt mixtures with low melting temperatures and high thermal stabilities for CSP applications [3]. Siegel et al presented measured thermophysical property data for several commercial and non-commercial molten salt mixtures that can be used in the system level design of parabolic trough and central receiver power plants [2]. Solid materials for high temperature thermal energy storage system in CSP have been widely investigated. Kenneth Guy Allen [6] investigated the rock type, properties, suitability and availability in rock bed storage system. It showed that the most suitable rock is likely to be igneous or metamorphic rock, without voids or minerals that will decompose when heated to temperatures of 500–600°C. A low-cost material inherited from the industrial vitrification of Asbestos was analysed as a good candidate of storage materials [4]. Quartzite rocks and sands were suitable to be used as the low-cost solid fillers which provided the bulk of thermal capacitance of the thermal storage [19].Yang and Garimella [12,13] carried out a series of numerical investigations on the molten-salt packed-bed thermocline system using the developed two-temperature model. Li et al. [15] presented dimensionless heat transfer governing equations for fluid and solid fillers for the packed-bed thermocline TES and studied various scenarios of thermal energy charging and discharging processes. Xu et al. [7,8,9] presented a transient two-dimensional dispersion-concentric model to investigate the discharging behavior of the packed-bed thermocline tank. A parametric analysis was carried out and various influencing factors were analyzed. Mario Biencinto developed a simulation model for solar thermal power plants with a thermocline storage tank with logistic function in TRNSYS, and assessed different operation strategies [5]. Most of the above studies were focused on evaluating the tank performance with a particular type of HTF and solid material under adiabatic conditions and the assumption of inlet plug flow. To the author's knowledge, there have been no studies regarding the evaluation of the thermocline TES system performance and the comparison of using different HTFs and different non-uniform inlet flow boundary conditions in the thermocline TES systems, though it is important to evaluate different materials in designing plants and how the system will perform in actual hardware with non-uniform inlet flow. In this study, a transient two-dimensional and two-temperature model is developed to investigate the heat transfer and fluid dynamics in a molten salt thermocline thermal storage system. After model validation, the effects of inlet flow boundary condition and storage medium properties including fluid and solid material on the thermal performance of thermocline storage system are investigated. With the chosen basic design parameters such as particle diameter, fluid and solid materials, the size of a 2MWh thermocline tank is determined by a simple one-dimensional design method.

2. Mathematical model

2.1. Governing equations

The general layout of the thermocline storage system is illustrated in Fig. 1.

The following assumptions are employed to simplify the analysis:

(1) The fluid flow and heat transfer are symmetrical about the axis.

(2) The distributors are not included in the computational domain and plug flow or assumed Hagen-Poiseuille flow is imposed at the inlet of the filler region.

(3) The flow of molten salt is laminar and incompressible.

(4) The solid fillers are spherical particles with the same diameter and constant properties.

Continuity equation:

$$\frac{\partial \varepsilon \rho_l}{\partial t} + \nabla \cdot (\rho_l \vec{v}) = 0 \tag{1}$$

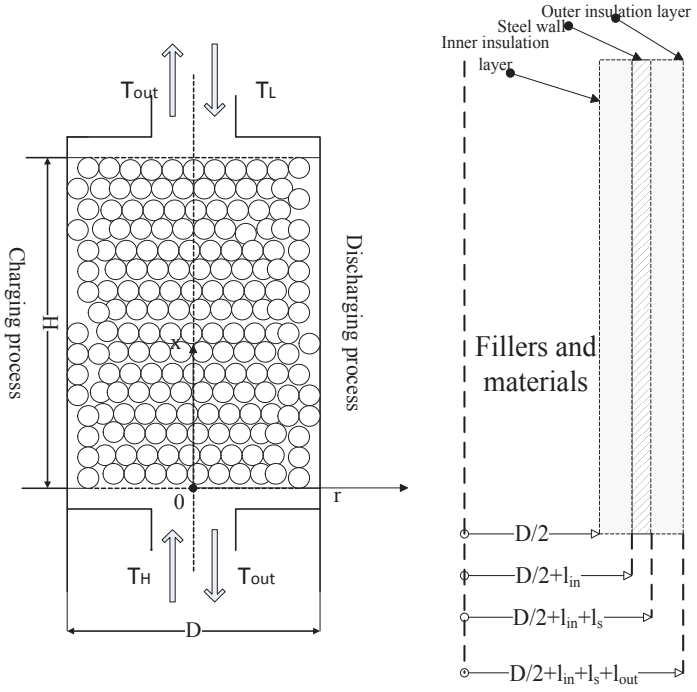

Fig.1. Schematic diagram of the molten salt thermocline TES and the computational domain.

Momentum equation:

$$\frac{\partial(\rho_l \vec{v})}{\partial t} + \nabla\cdot(\rho_l \frac{\vec{v}\vec{v}}{\varepsilon}) = -\varepsilon\nabla p + \nabla\cdot(\mu\nabla\vec{v}) + \varepsilon\rho_l \vec{g} + \varepsilon(\frac{\mu}{K} + \frac{F}{\sqrt{K}}\rho_l v_{mag})\vec{v} \tag{2}$$

where $K = \frac{d_p^2\varepsilon^3}{150(1-\varepsilon)^2}$, $F = \frac{1.75}{\sqrt{150\varepsilon^3}}$. In the axisymmetric coordinate system shown in Fig. 1, the problem is two-dimensional, incompressible fluid : $\nabla = \vec{e_r}\frac{\partial}{\partial r} + \frac{\vec{e_\theta}}{r}\frac{\partial}{\partial\theta} + \vec{e_x}\frac{\partial}{\partial x}$, $\vec{V} = v_r\vec{e_r} + v_x\vec{e_x}$.

As the volume expansion/shrinkage, viscous effects and kinetic energy changes the conduction or convection terms are omitted, Energy equation for the molten salt:

$$\frac{\partial(\varepsilon\rho_l C_{p,l}T_l)}{\partial t} + \nabla\cdot(\rho_l\vec{v}C_{p,l}T_l) = \nabla\cdot(k_{l,eff}\nabla T_l) + h_i(T_s - T_l) \tag{3}$$

Energy equation for the solid fillers:

$$\frac{\partial((1-\varepsilon)\rho_s C_{p,s}T_s)}{\partial t} = \nabla\cdot(k_s\nabla T_s) - h_i(T_s - T_l) \tag{4}$$

Energy equation for the insulation layers and tank steel wall:

$$\frac{\partial(\rho_i C_{p,i}T_i)}{\partial t} = \nabla\cdot(k_i\nabla T_i) \tag{5}$$

2.2. Boundary conditions and initial conditions

Boundary conditions are summarized in Table 1. At the beginning of the discharging process, it is assumed that the tank is filled with molten salt and solid fillers which have the same hot temperature, and the tank wall is in thermally equilibrium with the interior hot storage material and the outside ambient air with a velocity of 2m/s.

Table 1. Boundary conditions.

Number	Boundary conditions	
BC1: x=0, 0≤r<D/2;	$v_x\|_+ = v_{in}$, $v_r\|_+ = 0$, $T_f\|_+ = T_{f,in}$, $\partial T_s/\partial x\|_+ = 0$	bottom inlet
BC2: x=H, 0≤r<D/2;	$\partial v_x/\partial x\|_- = 0$, $v_r\|_- = 0$, $\partial T_f/\partial x\|_- = 0$, $\partial T_s/\partial x\|_- = 0$	top outlet
BC3: 0≤x≤H,r=0;	$\partial v_x/\partial r\|_+ = 0$, $r\|_+ = 0$, $\partial T_f/\partial r\|_+ = 0$, $\partial T_s/\partial r\|_+ = 0$	symmetry axis of the cylindrical tank
BC4: 0≤x≤H, r=D/2;	$v_x\|_- = v_r\|_- = 0$, $k_{f,eff}\,\partial T_f/\partial x\|_- = k_{in}\,\partial T_{in}/\partial r\|_+$, $k_{s,eff}\,\partial T_s/\partial r\|_- = 0$	the inner surface of the insulation inner layer
BC5: x=0 or x=H, D/2≤ r≤D/2+l_{in}+l_{out}+l_s;	$\partial T_{in}/\partial x = \partial T_s/\partial x = \partial T_{out}/\partial x = 0$	two cross sections of the insulation layers and tank steel wall adjacency to the fluid inlet and outlet
BC6: 0≤x≤H,r=D/2+l_{in}+l_{out}+l_s;	$-k_{out}\dfrac{\partial T}{\partial r}\Big\|_+ = h(T_{out} - T_\infty)$, $Nu = hH/k = 0.664\,\mathrm{Re}_D^{0.5}\,\mathrm{Pr}^{0.5}$, $\mathrm{Re}_D = \dfrac{v_{air}D}{\nu_{air}}$	outmost wall of the thermocline tank

where v_{air} and ν_{air} are the velocity and viscosity of ambient air, respectively.

2.3. Numerical method

The computational domain is discretized into finite volumes. All the variables are stored at the centers of the mesh cells. A second-order upwind scheme is used for the convective fluxes, while a central-differencing scheme is used for discretizing the diffusion fluxes. Iterations at each time step are terminated when the dimensionless residuals for all equations drop below 10^{-4}. The computations are performed using the commercial software FLUENT through the SIMPLEC algorithm. User-defined functions are developed to account for Eqs. (2-4). Grid and time-step dependence are checked by inspecting results from different grid densities and time intervals. Based on this, Δx=Δr=0.01m and Δt=0.5s are chosen as this setting results in a temperature along the line r=0 throughout the discharge process that is within 3% of that for the case with Δx=Δr=0.005m and Δt=0.1s.

3. Model validation

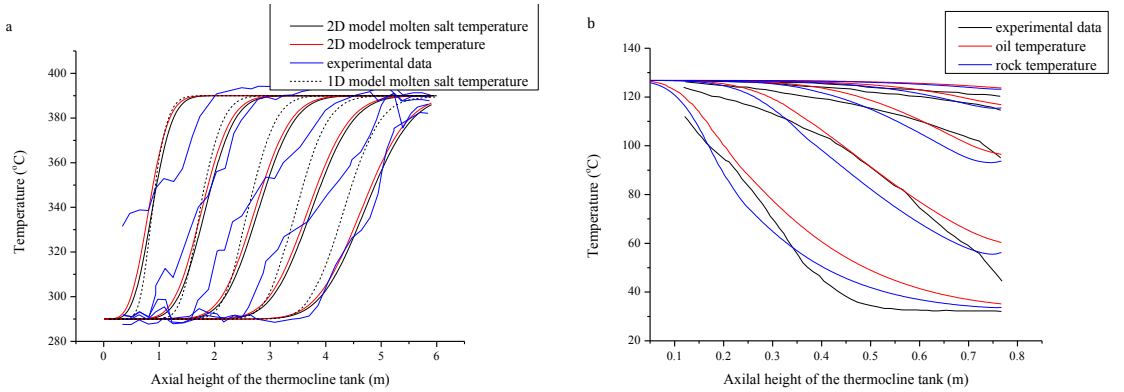

Fig. 2. (a). comparison between thermocline profiles from numerical results of both 2-D model and 1-D model [15] and experimental results from Ref. [10] in a discharging cycle of the molten salt tank at time intervals of 30 minutes; (b) comparison between the numerical and experimental charging temperature distribution along the oil tank height at time intervals of 16 minutes from Ref. [17]

It has been successfully validated with experimental data taken from the literatures.

4. Comparative analysis results and discussion

The results of thermocline tank design efforts are strongly tied to the parameters such as: thermophysical properties of the heat transfer fluid and thermal storage media, the design velocity in charging and discharging cycle. In this section we report the results of our ongoing efforts to characterize the effects of different commercial nitrate salt heat transfer fluids, different solid materials, different inlet velocity profiles. Other parameters and properties used in the model: H=5m, D=2m, l_{in}= l_{out}=0.1m, l_{st} =0.02m, porosity ε=0.22; k_{in}=0.1W/m·K, $k_{st,eff}$=35W/m·K.

4. 1. Different molten salts

There are several nitrate salt mixtures currently under consideration for use in CSP systems. In particular the binary system KNO_3-$NaNO_3$ ("Solar salt" system) is well known and has been widely used for TES systems, which is usually considered to be a mixture of 60 wt% $NaNO_3$ and 40 wt% KNO_3. Other ternary mixtures include KNO_3-$NaNO_2$-$NaNO_3$ (trade names include Hitec, Durferrit ASD, HTS) and $Ca(NO_3)_2$-KNO_3-$NaNO_3$ (trade name Hitec XL), which have been considered to replace the Solar Salt because of its low freezing point. The physical properties of three molten salts are listed in Table 2.

Table 2. Physical properties of molten salts.

Name	Solar slat [7-9] (60% $NaNO_3$, 40 % KNO_3)	Hitec [12] (7% $NaNO_3$, 53% KNO_3, 40% $NaNO_2$)	Hitec XL [2] (42% $Ca(NO_3)2$, 43% $NaNO_3$, 15% KNO_3)
Density (kg/m^3)	$\rho_l = 2090 - 0.636 \times T_l(^oC)$	$\rho_l = 2084 - 0.732 \times T_l(^oC)$	$\rho_l = 2240 - 0.827 \times T_l(^oC)$
Specific heat capacity (J/kg·K)	$Cp_l = 1443 - 0.172 \times T_l(^oC)$	$Cp_l = 1561.7$	$Cp_l = 1545.54456 - 0.33563 \times T_l(^oC)$
Thermal conductivity (W/m·K)	$k_l = 0.443 + 1.9 \times 10^{-4} \times T_l(^oC)$	$k_l = 0.421 - 6.53 \times 10^{-4}(T_l - 260)$	$k_l = 0.519$
Viscosity (kg/ms)	$\mu_l = [22.714 - 0.12 \times T_l(^oC) + 2.281 \times 10^{-4} \times T_l(^oC)^2 - 1.474 \times 10^{-7} \times T_l(^oC)^3] \times 10^{-3}$	$\mu_l = \exp[-4.343 - 2.0143 \times (\ln T_l - 5.011)]$	$\mu_l = 10^{6.1374} \times T_l^{-3.36406}(^oC)$
Melting point (°C)	221	142	130-140
Stability limit (°C)	600	450-538	550

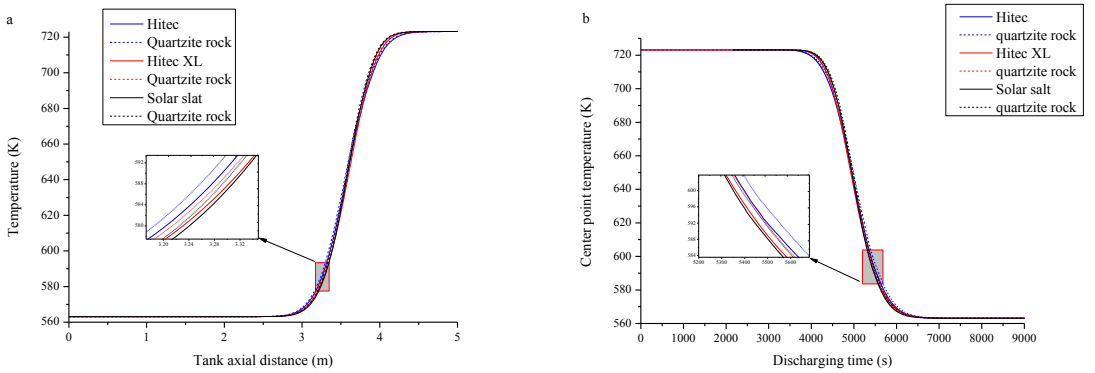

Fig.3. (a) Variations in temperature profiles of HTF and quartzite rock at 7200s along the centerline of tank axial distance for different molten salts; (b) center point temperature profiles with the discharging time for different molten salts

Fig.3 shows that solar salt has the sharpest temperature gradient with tank axial distance (Fig.3.a) and quickest cooling rate in the center point of the tank (Fig.3.b). Temperature differences between centerline and near-wall area, solid and fluid are both very small (0.05K).

Thermocline thickness is defined as the covering length of the thermocline region and can be expressed as: $\min\{H(T_{out}), H(T_{crit,h})\} - H(T_{crit,c})$ in discharging cycle and $H(T_{crit,h}) - \max\{H(T_{out}), H(T_{crit,c})\}$ in charging cycle, where $T_{crit,h} = T_h - 5$ and $T_{crit,c} = T_c + 5$ represent the critical low and hot temperatures for evaluating the thermocline thickness, respectively.

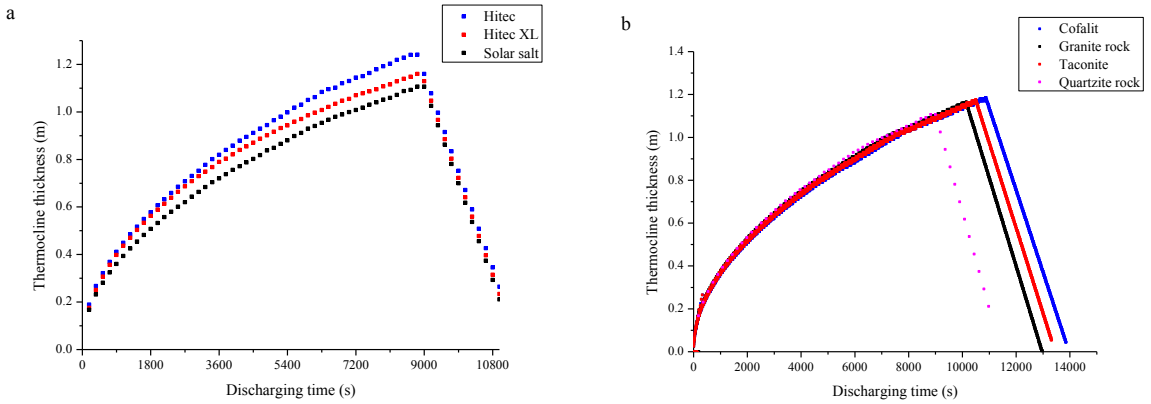

Fig.4. (a) The thermocline thickness with the discharging time for different molten salts; (b) The thermocline thickness with the discharging time for different solid materials.

Fig.4.a shows the change of thermocline thickness with discharging time is similar for different molten salts, while thermocline movement velocity is different. Solar salt tank has the smallest and slowest thermoclne thickness. So solar salt is best as HTF of thermocline TES system.

4.2. Different solid materials

Properly specifying and qualifying the filler material as a significant component of this system is a major element for both first-cost and long-term maintenance costs associated with TES systems. The effect of solid material on the system performance is investigated through testing four promising thermal storage materials. The physical properties of these solid materials are summarized in Table 3.

Table 3. Physical properties of solid materials.

Solid material	Density (kg/m^3)	Average specific heat capacity (J/kg·K)	Thermal conductivity (W/m·K)	Price ($/t)
Quartzite rock[7-9]	2500	830	5.69	$11.2/t
Rock(granite) [6]	2893	845	3.0	$47.0/t
Taconite[16]	3200	800	30	$200/t
Cofalit®[4]	3120	860	2.7	$11.1/t

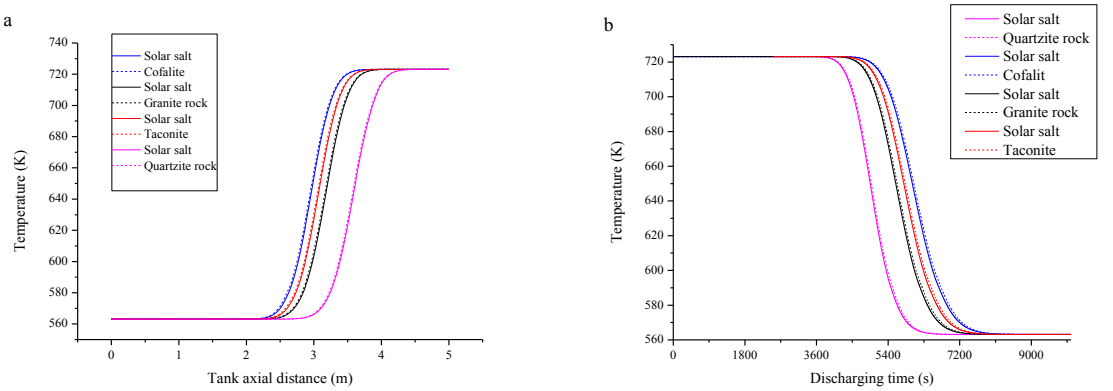

Fig.5. (a) Variations in temperature profiles of HTF and solid material at 7200s along the centerline of tank axial distance for different solid materials; (b) center point temperature profiles with the discharging time for different solid materials

Fig.5 shows that thermocline tank still has the largest stored energy after same discharging time (Fig.5.a) and the longest discharging time (Fig.5.b) with Cofalit® as solid material, while both of them are the smallest for quartzite rock. It is because the volumetric heat capacity is different for different solid materials. Larger volumetric heat capacity solid material stores larger total energy. It also shows that temperature difference between HTF and solid is smaller for larger thermal conductivity solid material.

Fig.4.b shows the thermocline thickness increases slower for larger volumetric heat capacity solid material before the peak, as it can be seen that the thermocline thicknesses are close but smaller for larger volumetric heat capacity solid material at the same discharging time, while the peak of thermocline thickness is larger because the larger discharging time. Generally speaking, the Cofalit® is best for thermocline heat storage solid material with 29.31% larger in the volumetric heat capacity and only 9.09% larger in the largest thermocline thickness compared with quartzite rock, but the quartzite rock is still chosen as solid material in the design as it is much more available.

4.3. Different velocity profiles

Usually, a uniform distribution of the flow through the whole cross section of the inlet and outlet (plug flow) is assumed in the simulations of thermocline tank system with two distributor regions included at the upper and lower ends of the filler region in the storage tank. However, the idealized flow with complete mixing in the radial direction is hard to achieve in actual applications because the edge effect and difficulties in sophisticated-designed distributor. The inlet flow boundary condition of non-uniform velocity profile, as would be found in actual applications were not explored. So the effect is evaluated with Hagen-Poiseuille flow instead of plug flow as the inlet flow boundary condition, which forms one of the focus of the present study. Three different parabolic velocity profiles are assumed: $V = V_{\max}(1-\frac{r^2}{R^2})$, $V_{\max} = 4.186\times10^{-4}, 8.372\times10^{-4}, 1.256\times10^{-3}$ m/s for case V1, V2, V3; respectively. The non-uniformity and mass flow rate are both V3>V2>V1.

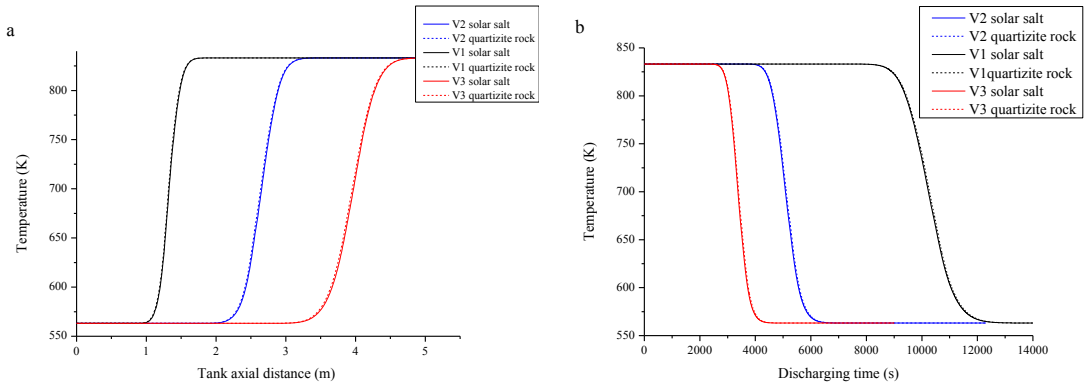

Fig.6. (a) Variations in temperature profiles of HTF and solid material at 7200s along the centerline of tank axial distance for different inlet velocity profiles; (b) center point temperature profiles with the discharging time for different inlet velocity profiles.

Fig.6 shows that the temperature gradient in axial distance at the same time and discharging time are both larger with smaller V_{max}, while the thermocline movement velocity and cooling rate in the center of thermocline tank in discharging time is smaller.

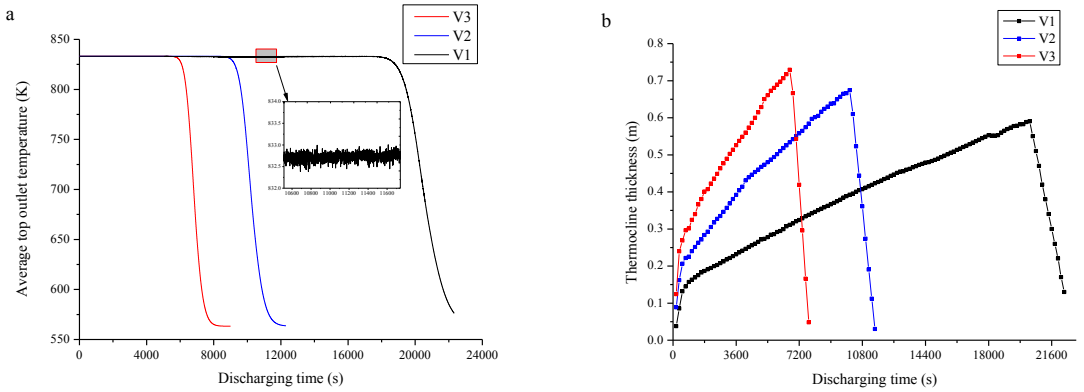

Fig.7. (a) Variations in the average top outlet temperature with the discharging time for different inlet velocity profiles; (b) thermocline thickness with the discharging time for different inlet velocity profiles.

Fig.7 shows that the thermocline thickness increases slower and the largest thermocline thickness is smaller with smaller V_{max}, which means the thermocline thickness increases with the non-uniformity of inlet velocity boundary condition. For V1 case, the smaller V_{max} causes larger fluctuations in average outlet temperature. It is because the inlet non-uniform flow is still not fully mixed in radial direction after flowing the porous media in the tank with small V_{max}. It illustrates that the uniform inlet flow is better than any non-uniform flow for thermocline tank with the same mass flow rate. It can be concluded that smaller intlet mass flow rate is better for the thermocline storage tank, while it also causes smaller discharging power, and the well-designed distributor is very important. Any motion in the second or third directions would only enhance mixing and widen the thermocline appreciably. The mixing during charge and discharge cycles is one of the major contributors to the loss of thermodynamic availability of stored energy.

4.4 Design method and results

With the chosen basic design parameters: P=1MW, T_{dc}=2h, solar slat and quartzite rock as HTF and solid material, respectively. Solid filler d_s=1.9cm, porosity ε =0.22, Working temperature range: 290°C-560°C. The

design inlet velocity is 4.186×10^{-4} m/s. The size of a 2MWh thermocline tank is determined by simple one-dimensional design models [15, 20], validated by single phase one dimensional model (CIEMAT1D1SF) [21]. Then the normalized tank dimensions included in the standards are taken into account, in which H/D ratio for tanks with D<5 m should be between 1.5 and 4 [21]. The results of design cases are summarized in Table 4.

Table 4. Design cases.

Design case	D	H	Discharge efficiency	H/D ratio
1	1.6	7.4593	0.8339	4.662
2	1.7	6.6489	0.8287	3.9111
3	1.8	5.9673	0.8236	3.3152
4	1.9	5.3885	0.8186	2.8360
5	2.0	4.8924	0.8137	2.4462
6	2.1	4.4640	0.8089	2.1257
7	2.2	4.0912	0.8042	1.8597
8	2.3	3.7649	0.7996	1.6369
9	2.4	3.4774	0.7950	1.4489

Where $\eta = \dfrac{\int_0^{T_{dc}} \dot{m} C_p (T_{out} - T_c) dt}{Q_{store}}$, $T_{out} > T_c + 0.95(T_h - T_c)$.

It shows that the design tank sizes in case 2-8 are feasible. Tank with larger H/D ratio has higher discharge efficiency.

5. Conclusion

In this study, a transient two-dimensional and two-temperature model is developed to investigate the heat transfer and fluid dynamics in a molten salt thermocline thermal storage system. After model validation, the effects of inlet flow boundary condition and storage medium properties including fluid and solid material on the thermal performance of thermocline storage system are investigated. With the chosen basic design parameters such as particle diameter, fluid and solid materials, the size of a 2MWh thermocline tank is determined by a simple one-dimensional design method.

(1)Thermoclne thickness increases slowest with solar salt as HTF. So solar salt is best as HTF in the thermocline storage system.

(2) Cofalit® is best for thermocline heat storage solid material with 29.31% larger in the volumetric heat capacity and only 9.09% larger in the largest thermocline thickness compared with quartzite rock.

(3) Smaller mass flow rate is better for the thermocline storage tank even with non-uniform inlet flow boundary condition, while it also causes smaller discharging power. Any non-uniformity of inlet flow or motion in the second or third directions would only enhance mixing and widen the thermocline appreciably, which contributors to the loss of thermodynamic availability of stored energy. Smaller non-uniformity of inlet flow is better though it may causes larger fluctuations in average outlet temperature.

(4) Thermocline heat storage tank with larger H/D ratio has higher discharge efficiency.

Acknowledgement

This work is supported by the National Natural Science Foundation of China (51106149), the Beijing Municipal Science & Technology Commission (D121100001012001), and the China National Hi-Tech R&D (863 Plan) (2013AA050502).

References

[1] Electric Power Research Institute. Solar Thermocline Storage Systems: Preliminary Design Study. Palo Alto, CA (2010) 1019581.
[2] Siegel, N.P., Bradshaw, R.W., Cordaro, J.B., et al. Thermophysical Property Measurement of Nitrate Salt Heat Transfer Fluids, in ASME 5th International Conference on Energy Sustainability, 2011, ASME: Washington, D.C., USA.
[3] Bauer, T., Laing, D. and Tamme, R. Recent Progress in Alkali Nitrate/Nitrite Developments for Solar Thermal Power Applications, Molten Salts Chemistry and Technology, MS9, Trondheim, Norway, 2011.
[4] X. Py, N. Calvet, R. Olivès, P. Echegut, C. Bessada, F. Jay. Thermal storage for solar power plants based on low cost recycled material. EFFSTOCK, the 11th International Conference on Thermal Energy Storage, June 14-17, 2009, Stockholm, Sweden.
[5] Mario Biencinto,Rocio Bayon , Esther Rojas , Lourdes Gonzalez . Simulation and assessment of operation strategies for solar thermal power plants with a thermocline storage tank, solar energy 2014;103: 456-72.
[6] Kenneth Guy Allen. Rock bed thermal storage for concentrating solar power plants, Stellenbosch University, dissertation for Ph.d degree.
[7] Xu C, Li X, Wang ZF, He YL, Bai FW. Effects of solid particle properties on the thermal performance of a packed-bed molten-salt thermocline thermal storage system. Applied Thermal Engineering 2013;57: 69-80.
[8] Xu C, Wang ZF, He YL, Li X, Bai FW. Sensitivity analysis of the numerical study on the thermal performance of a packed-bed molten salt thermocline thermal storage system. Applied Energy 2012;92: 65-75.
[9] Xu C, Wang ZF, He YL, Li X, Bai FW. Parametric study and standby behavior of a packed-bed molten salt thermocline thermal storage system. Renew Energy 2012;48:1-9.
[10] Pacheco JE, Showalter SK, Kolb WJ. Development of a molten-salt thermocline thermal storage system for parabolic trough plants. In: Proceedings of solar forum 2001 solar energy: the power to choose. Washington, DC; 21-25 April 2001.
[11] Valmiki MM, Karaki W, Li P, Lew JV, Chan C, Stephens J. Experimental investigation of thermal storage processes in a thermocline tank. J Solar Energy Eng 2012;134: 041003.
[12] Yang Z, Garimella SV. Molten-salt thermal energy storage in thermoclines under different environmental boundary conditions. Applied Energy 2010;87: 3322-9.
[13] Yang Z, Garimella SV. Cyclic operation of molten-salt thermal energy storage in thermoclines for solar power plants. Applied Energy 2013;103: 256-65.
[14] Flueckiger SM, Garimella SV. Second-law analysis of molten-salt thermal energy storage in thermoclines. Solar Energy 2012;86:1621-31.
[15] Li P, Lew JV, Karaki W, Chan C, Stephens J, Wang Q. Generalized charts of energy storage effectiveness for thermocline heat storage tank design and calibration. Solar Energy 2011;85: 2130-43.
[16] Peiwen Li , Jon Van Lew, Cholik Chan, et al. Large Capacity Heat Storage for Extended Operation of a Solar Thermal Power Plant, The University of Arizona. http://www.azrise.org/wp-content/uploads/2012/12/Large-Capacity-Heat-Storage.pdf
[17] M. M. Valmiki, Wafaa Karaki, Peiwen Li, et al. Experimental Investigation of Thermal Storage Processes in a Thermocline Tank. Journal of Solar Energy Engineering 2012; 134(4), 041003.
[18] Anish Modi, Carlos David Perez-Segarra.Thermocline thermal storage systems for concentrated solar power plants: One-dimensional numerical model and comparative analysis. Solar Energy 2014; 100:84-93.
[19] Brosseau D, Kelton JW, Ray D, Edgar M, Chisman K, Emms B. Testing of thermocline filler materials and molten-salt heat transfer fluids for thermal energy storage systems in parabolic trough power plants. J Solar Energy Eng 2005; 127:109–16.
[20] Yang Z, Garimella SV. Thermal analysis of solar thermal energy storage in a molten-salt thermocline. Solar Energy 2010; 84:974-85.
[21] R. Bayon, E. Rojas. Simulation of thermocline storage for solar thermal power plants: from dimensionless results to prototypes and real size tanks, Int. J. Heat Mass Transfer 2013; 60:713–21.